Influence of the Structure of Drug Moieties on the *in Vitro* Efficacy of HPMA Copolymer–Geldanamycin Derivative Conjugates

Yuji Kasuya,,[1] Zheng-Rong Lu,[1] Pavla Kopečková,[1,2] S. Esmail Tabibi,[3] and Jindřich Kopeček[1,2,4]

Received October 17, 2001; accepted November 1, 2001.

Purpose. To optimize the structure of geldanamycin (GDM) derivative moieties attached to N-(2-hydroxypropyl)methacrylamide (HPMA) copolymers via an enzymatically degradable spacer.

Methods HPMA copolymers containing different AR-GDM (AR = 3-aminopropyl (AP), 6-aminohexyl (AH), and 3-amino-2-hydroxypropyl AP(OH)) were synthesized and characterized. Their cytotoxicity towards the A2780 human ovarian carcinoma cells was evaluated.

Results The cytotoxic efficacy of HPMA copolymer-AR-GDM conjugates depended on the structure of AR-GDM. Particularly, HPMA copolymer-bound AH-GDM, which possessed the longest substituent at the 17-position, demonstrated the highest efficacy among the polymer-bound GDM derivatives; however the activity of free AH-GDM was lower than that of the other free AR-GDMs. The relative increase of the activity of macromolecular AH-GDM when compared to AP-GDM or AP(OH)-GDM correlated with the enhanced recognition of AH-GDM terminated oligopeptide side-chains by the active site of the lysosomal enzyme, cathepsin B. Drug stability and further stabilization upon binding to HPMA copolymer also contributed to the observed phenomena.

Conclusions AH-GDM was found to be a suitable GDM derivative for the design of a drug delivery system based on HPMA copolymers and enzymatically-degradable spacers.

KEY WORDS: geldanamycin; N-(2-hydroxypropyl)methacrylamide copolymers; ovarian carcinoma; drug delivery system; aqueous two phase system; cathepsin B.

INTRODUCTION

Geldanamycin (GDM), a benzoquinone ansamycin antibiotic, is a heat shock protein inhibitor (1,2). It inhibits the capacity of heat shock proteins such as HSP-90 and GRP-94 to form complexes with client oncoproteins. It is expected that geldanamycin will be developed as an anticancer drug based on the new mechanism of action. Furthermore, recent biological evaluations have revealed the effectiveness of the combination chemotherapy of GDM with other cytotoxic agents such as doxorubicin and paclitaxel (3). On the other hand, to overcome toxicity problems observed during preclinical evaluation (4), GDM delivery systems have been designed and studied (5–7).

Attachment of anticancer drugs via lysosomally degradable spacers (e.g., the GFLG oligopeptide sequence) to water soluble drug carriers, such as N-(2-hydroxypropyl)methacrylamide (HPMA) copolymers results in an increased therapeutic efficacy (8,9). Generally, water soluble macromolecules preferentially accumulate in solid tumors by the enhanced permeation and retention (EPR) effect (10). Lysosomally degradable oligopeptide spacers ensure the stability of the conjugates during transport and efficient drug release after endocytosis of conjugates (11,12). Moreover, the unique internalization and subcellular trafficking of macromolecular drugs result in a modified mechanism of drug action, when compared to low molecular weight drugs (9,13).

For conjugation with drug carriers, the methoxy group on the 17-position of GDM has been substituted with several diaminoalkanes to introduce the reactive primary amino group (5–7,14). Previously, we synthesized and evaluated HPMA copolymer-GDM derivative conjugates using 17-(3-aminopropylamino)-17-demethoxygeldanamycin (AP-GDM) (5). On the other hand, antibody-GDM derivative conjugates have been synthesized using AP-GDM and 17-(4-aminobutylamino)-17-demethoxygeldanamycin (5,6). However, the structure of the 17-substituent has not been optimized from the viewpoint of the efficacy. The objective of this study was to evaluate the influence of the structure of drug moieties on the efficacy of HPMA copolymer-GDM derivative conjugates. Several 17-substituted GDM derivatives (AR-GDM, AR = 3-aminopropylamino, AP; 6-aminohexylamino, AH; and 3-amino-2-hydroxypropylamino, AP(OH)) were synthesized and attached to HPMA copolymers. The HPMA copolymer-GDM derivative conjugates were characterized and their *in vitro* efficacy towards the A2780 human ovarian carcinoma cells evaluated. The data were correlated with the stability of the drugs and conjugates, their hydrophobicity, and rate of AR-GDM release by lysosomal cysteine proteinase, cathepsin B.

MATERIALS AND METHODS

Chemicals

GDM was kindly supplied by the National Cancer Institute. HPMA (15), N-methacryloylglycylglycine p-nitrophenylester (16) (MA-GG-ONp), and N-methacryloylglycylphenylalanylleucylglycine p-nitrophenylester (17) (MA-GFLG-ONp) were synthesized as described previously. Cathepsin B (28 U/mg proteins) from bovine spleen and its standard substrate, N-benzoyl-Phe-Val-Arg-p-nitroanilide hydrochloride, were purchased from Sigma (St. Louis, Missouri). Dextran T-500 was purchased from Pharmacia Biotech (Piscataway, New Jersey). Other chemicals were of reagent grade and used without further purification.

[1] Department of Pharmaceutics and Pharmaceutical Chemistry/CCCD, University of Utah, Salt Lake City, Utah 84112.
[2] Department of Bioengineering, University of Utah, Salt Lake City, Utah 84112.
[3] Pharmaceutical Resources Branch, National Cancer Institute, NIH, Bethesda, Maryland 20892-7446.
[4] To whom correspondence should be addressed. (e-mail: Jindrich.Kopecek@m.cc.utah.edu)

ABBREVIATIONS: AH, 6-aminohexylamino; AP, 3-aminopropylamino; AP(OH), 3-amino-2-hydroxypropylamino; AR, aminoalkylamino; AR-GDM, 17-(AR)-17-demethoxygeldanamycin; GDM, geldanamycin; HPMA, N-(2-hydroxypropyl)methacrylamide; MA-GFLG-, N-methacryloylglycylphenylalanylleucylglycyl; MA-GG-, N-methacryloyglycylglycyl; -ONp, p-nitrophenylester; P-(AR-GDM), HPMA copolymer-AR-GDM conjugate; PEG, Poly(ethylene glycol); SE, standard error.

Synthesis and Characterization of AR-GDMs and MA-GFLG-AR-GDMs

The synthesis of GDM derivatives and the structure of HPMA copolymer-AR-GDM conjugates are shown in Scheme 1. AR-GDM (AR-GDM · HCl) and MA-GFLG-AR-GDM were synthesized as described previously (5,12). Briefly, various diaminoalkanes were reacted with GDM to obtain AR-GDMs. Then, AR-GDMs were coupled with MA-GFLG-ONp.

To determine the partition coefficient, AR-GDM · HCl was dissolved in n-octanol at 10 μM, and the solution was mixed with PBS (5 mM Na_2HPO_4, 150 mM NaCl, pH 6.5 or 7.4) at the volume ratio, 1/1. The drug concentrations in aqueous and organic layers were measured spectrophotometrically at 332 nm. Partition coefficient was calculated as the ratio of the [concentration in the organic layer /[concentration in the aqueous layer].

For the structure validation of GDM derivatives, mass spectroscopy was carried out using a mass spectrometer Voyager-DE (STR Biospectrometry Workstation, PerSeptive Biosystem, Inc., Framingham, MA), elemental analysis by Atlantic Microlab, Inc., Norcross, GA, and two-dimensional NMR using a spectrometer Varian Unity 500 MHz and dimethylsulfoxide-d_6 as a solvent. For AH-GDM · HCl, Rf = 0.43 on silica gel and AcOEt/MeOH (2/1); m/e = 645.2 (M^+ + 1 for AH-GDM (free base), M = 645.8); elemental analysis calculated for AH-GDM · HCl · $2H_2O$

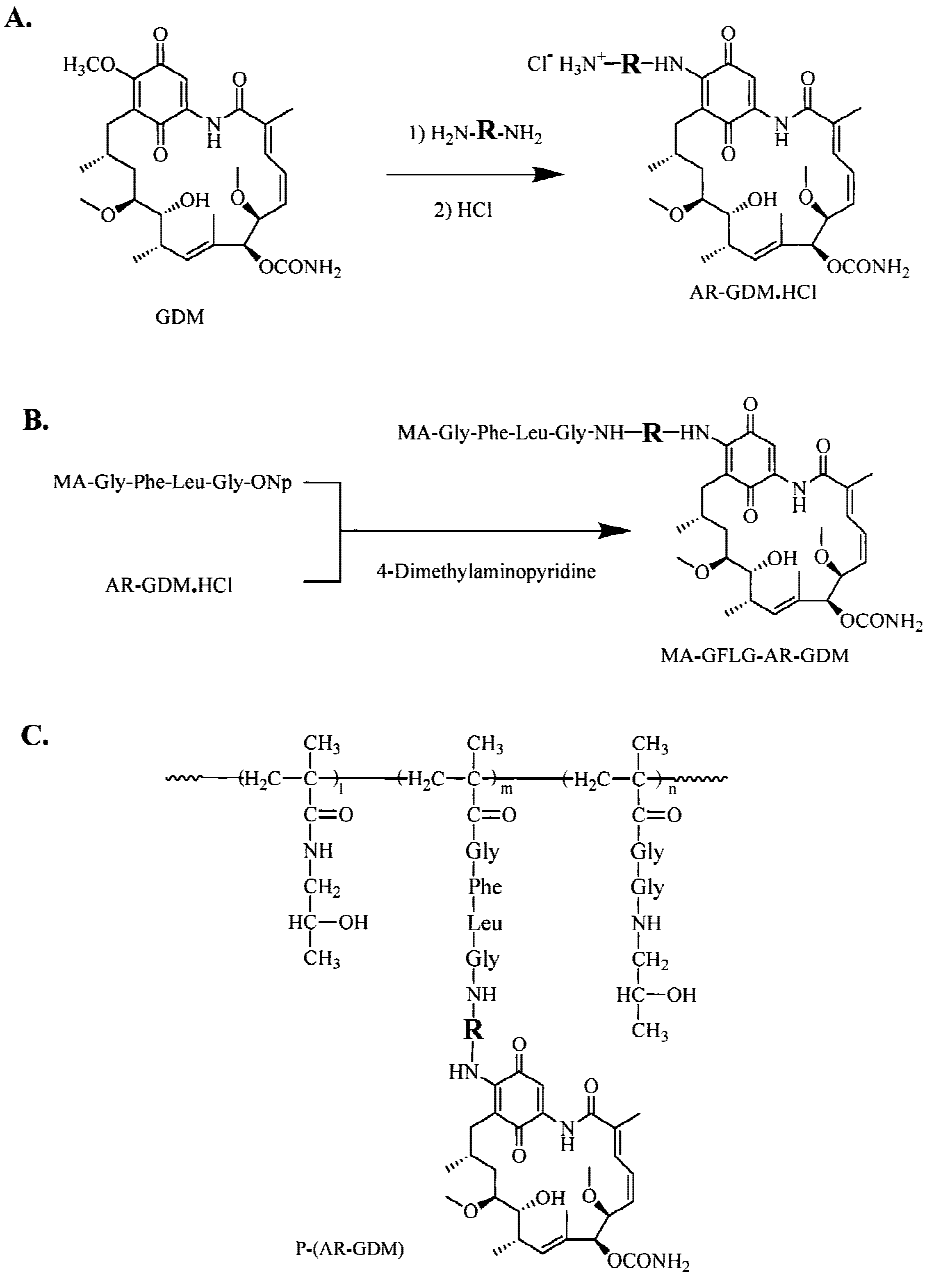

Scheme 1. Synthesis of various GDM derivatives and their conjugation with HPMA copolymers. A. Synthesis of AR-GDM. -R- = $-(CH_2)_3-$ (AP), $-(CH_2)_6-$ (AH), and $-CH_2-CH(OH)-CH_2-$(AP(OH)). B. Conversion of AR-GDM to MA-GFLG-AR-GDM. C. Structure of P-(AR-GDM).

($C_{34}H_{53}O_8N_4Cl \cdot 2H_2O$; C, 56.93; H, 8.01; N, 7.81; found: C, 56.73; H, 7.62; N, 7.71. For MA-GFLG-AH-GDM, Rf = 0.78 on silica gel and AcOEt/MeOH (2/1); m/e = 1085.7 (M – 1 (negative), M = 1087.3); elemental analysis calculated for MA-GFLG-AH-GDM $\cdot$ $2H_2O$ ($C_{57}H_{82}O_{13}N_8 \cdot 2H_2O$; C, 60.94; H, 7.72; N, 9.97; found: C, 60.91; H, 7.52; N, 9.73. For MA-GFLG-(AP(OH)-GDM, Rf = 0.79 on silica gel and AcOEt/MeOH (2/1); m/e = 1059.5 (M – 1 (negative), M = 1061.2); Anal. calcd. for MA-GFLG-AP(OH)-GDM $\cdot$ $2H_2O$ ($C_{54}H_{76}O_{14}N_8 \cdot 2H_2O$; C, 59.12; H, 7.35; N, 10.21; found: C, 59.41; H, 7.23; N, 10.36. Two-dimensional NMR assignments for these compounds are shown in the Appendix. The structure validations of the other GDM derivatives (AP-GDM, MA-GFLG-AP-GDM, and AP(OH)-GDM) have been reported previously (7,14).

Synthesis and Characterization of HPMA Copolymer-GDM Derivative Conjugates (P-(AP-GDM)s)

The polymers were prepared and characterized as described previously (7). Radical precipitation copolymerization of HPMA, MA-GFLG-(AR-GDM), and MA-GG-ONp was performed in acetone, using 2,2′-azobisisobutyronitrile as the initiator. The AR-GDM and ONp contents were determined spectrophotometrically after aminolysis of p-nitrophenylester groups with 1-aminopropan-2-ol, using $\varepsilon^{332nm} = 2.2 \times 10^4\ M^{-1}\ cm^{-1}$ in PBS and $\varepsilon^{410nm} = 1.8 \times 10^4\ M^{-1}\ cm^{-1}$ in 0.1 M aqueous NaOH as the molar extinction coefficients of AR-GDM and the p-nitrophenolate anion, respectively. Molecular weight was estimated by size exclusion chromatography. For the other characterizations and evaluations, p-nitrophenylester groups on the polymers were aminolyzed in the same way, and the polymers were purified with Sephadex G-25 (Pharmacia Biotech) using distilled water, freeze-dried, and stored in a freezer (–30°C).

The partition coefficient in aqueous two-phase system was determined as described previously (18) with minor modifications. Poly(ethylene glycol) $(PEG)_{6000}$ (5.05 g) and dextran T-500 (5.05 g) were dissolved in 100 mL of PBS (10 mM Na_2HPO_4, 150 mM NaCl, pH 7.4) or phosphate buffer (110 mM Na_2HPO_4, pH 7.4). The solution was allowed to stand overnight for the phase separation. Upper and lower phases were isolated and stored as stock solutions. Polymer solutions containing 4 mM AR-GDM moiety in distilled water were prepared using the freeze-dried samples. The upper and lower stock solutions and the polymer solution were mixed at the volume ratio of 0.99/0.99/0.02. The mixture was shaken vigorously and then allowed to stand for 30 min. The upper and lower phases were isolated and their polymer contents were determined from AR-GDM contents measured spectrophotometrically. The partition at the interface was calculated from the total AR-GDM contents and those partitioned into upper and lower phases.

Determination of IC_{50} Doses

IC_{50} dose was determined as described previously (7,19). The A2780 human ovarian carcinoma cell line was a gift from Dr. T. C. Hamilton (Fox Chase Cancer Center). The cells were cultured in RPMI-1640 medium containing 10% fetal bovine serum and 10 μg/mL insulin and grown at 37°C in a humidified atmosphere of 5% (CO_2 (v/v) in air. All experiments were performed on cells in the exponential growth phase. Cells seeded into a 96-well microtiter plate at 10,000 cells per well were incubated with drug solutions for 72 h. After the drug solution was discarded from each well, the fresh medium (100 μL) and a 5 mg/mL 3-(4,5-dimethylthiazol-2-yl)-2,5-diphenyltetrazolium bromide (Fluka, Buchs, Switzerland) solution (25 μL, medium: Dulbecco's phosphate buffered saline, (Sigma, St. Louis, Missouri) were added. Plates were incubated under the cell culture conditions for 3 h. The solution of 50% (v/v) dimethylformamide in water containing 20% (w/v) sodium dodecylsulfate (100 μL) was added to each well and the incubation was continued overnight. The absorbance of each sample was measured at 570 nm with a background correction at 630 nm. IC_{50} doses were determined from the drug concentration—cell viability curves using the following equation:

$$Y = Y_0 + (Y_m - Y_0)/(1 \times C/C_0)$$

where C_0 is the IC_{50} dose; Y the optical density in a well containing a particular drug concentration C; Y_m the optical density which corresponds to 100% cell viability; and Y_0 the optical density, which corresponds to 0% viability. From each series of the drug concentration—cell viability data, IC_{50} dose was determined by the least square method.

The drug solutions used above were prepared as follows. The freeze-dried P-AR-GDM or AR-GDM was first dissolved in dimethylsulfoxide [0.5% (v/v) of the final drug solution]. The solution was then diluted with cell medium to obtain the required solutions. Preliminary experiments showed that such a concentration of dimethylsulfoxide did not have a significant effect on the cell growth.

Evaluation of the Stability of Free and Polymer-Bound AR-GDMs

Free AR-GDMs were dissolved in PBS (10 mM Na_2HPO_4, 150 mM NaCl, pH 7.4) at 8 μM. The absorbance of the solution was measured at 332 nm over time. The decrease of the absorbance was used to calculate the concentration of AR-GDM remaining in the solution. We have reported that the main degradation mechanism of AP-GDM and AP(OH)-GDM is the intramolecular imine formation (cyclization) involving 3′-amino and 18-carboxyl groups (14). The cyclized products were found to have 47% smaller molar extinction coefficient than AP-GDM at 332 nm. The molar extinction coefficient of AH-GDM was also decreased to 47% in alkaline media that enhance the cyclization of AP-GDM and AP(OH)-GDMs although its degradation mechanism has not been identified yet.

Polymer-bound AR-GDMs were dissolved and incubated in PBS in the same way. After the incubation, the solution was applied to Sephadex G-25 column. The absorbance of the polymer fraction was measured at 332 nm. Because the primary amino group that induces the degradation was protected by the conjugation, we considered that the stability of the AR-GDM moiety could be evaluated from this absorbance, assuming that drug moiety is not decomposed until it is released from the polymer.

Evaluation of the Drug Release from P(-AR-GDM) Catalyzed by Cathepsin B

PBS (pH 7.4) consisting of 20 mM Na_2HPO_4, 150 mM NaCl and 5 mM ethylenediaminetetraacetic acid was pre-

pared as a medium. The stock solutions of cathepsin B (10 μM) and GSH (250 mM) in PBS, and the stock solutions of the standard substrate (N-benzoyl-Phe-Val-Arg-p-nitroanilide hydrochloride, 100 mM) and P-(AR-GDM) (4 mM of AR-GDM moiety) in DMSO were prepared. For the evaluation, the stock solutions of cathepsin B (360 μL), and GSH (24 μL) were added to PBS (798 μL) and incubated at 37°C for 10 min. To this solution was added the P-(AR-GDM) stock solution (18 μL). The mixture was incubated at 37°C for 1 h. An aliquot (500 μL) was taken and applied to the Sephadex G-25 column. The polymer fraction was collected and its drug content was determined at 332 nm. The amount of drug release was calculated from the drug contents before and after the incubation. The solution of standard substrate was used to verify the enzyme activity for each experiment.

Statistical Analysis

Data obtained were analyzed using F-test to compare the population variances and Student's or Welch's T-test was applied to compare the difference between two population means based on the results of F-test.

RESULTS AND DISCUSSION

Synthesis and Characterization of AR-GDMs and P-(AR-GDM)s

The partition coefficient of AR-GDM in n-octanol and buffers (pH 7.4 or 6.5) was determined to estimate the hydrophobicity of the drug molecules in physiological (pH 7.4) and lysosomal (more acidic than pH 7.4) conditions. Log (partition coefficient) of AP-GDM, AH-GDM, and AP(OH)-GDM were 0.30, 0.66, and 0.30 (pH 7.4); 0.16, 0.26, and 0.15 (pH 6.5), respectively. These results indicate that all AR-GDMs were moderately hydrophobic; AH-GDM was slightly more hydrophobic than AP-GDM and AP(OH)-GDM. It was the main structure of GDM that strongly affected the hydrophobicity of AR-GDM, and the different 17-substituents had only minor influences.

Various P-(AR-GDM)s were synthesized and characterized as shown in Table I. MA-GG-ONp was incorporated as a chain transfer agent to control (reduce) the molecular weight. As a result, the molecular weights of all polymers synthesized were below the renal threshold (approx. 45 kD for HPMA copolymers (20)). This relatively low molecular weight could avoid the unpredictable long-term disposition of polymer-drug conjugates in the body although higher molecular weight is favorable for the long circulation in the blood (20). The MA-GFLG-AR-GDM content in the copolymers could be controlled by changing the composition of the monomer mixture. Maximum drug content in the copolymers was estimated to be between 1.4–2.2 mol% as limited by the water solubility of the conjugates. Similar drug contents and molecular weights in Polymers 1, 4, and 5 were desirable to discuss the influence of the structure of drug moiety on the efficacy of P-(AR-GDM). Similar molecular weights and the same drug structure in Polymers 1 and 2 enabled to evaluate the influence of drug content as well.

Cytotoxic Efficacy of AR-GDMs and P-(AR-GDM)s

The IC_{50} doses for AR-GDM and P-(AR-GDM) are shown in Table II. All free AR-GDMs demonstrated cytotoxic activity towards A2780 cells. The efficacy was in the following order:

AP-GDM > AP(OH)-GDM > AH-GDM.

All HPMA copolymer-bound AR-GDMs demonstrated a higher IC_{50} value than corresponding free AR-GDMs (Table II). Such an increase in the IC_{50} dose may have resulted from the change of the main mechanism of cell entry: simple diffusion for low molecular weight drugs and endocytosis for polymeric drugs as already proved with HPMA copolymer-doxorubicin conjugates (9,13). This results in different intracellular concentration when cells are incubated with the same dose of free and polymer-bound drugs. Higher IC_{50} doses usually mean less effectiveness of the drug. However, as indicated above, macromolecular therapeutics may have a modified mechanism of drug action that results in the rationality of their use. In addition, if the activity of low molecular

TABLE I. Characteristics of HPMA Copolymer–Geldanamycin Derivative Conjugates*

Polymer. no.	Structure	AR-GDM content[b] (mol%)	ONp content[c] (mol%)	Molecular weight[d]	Solubility in PBS
1	P-(AP-GDM)	0.7	3.1	17,200 (M_w/M_n = 1.2)	soluble
2	P-(AP-GDM)	1.4	2.4	17,900 (M_w/M_n = 1.2)	soluble
3	P-(AP-GDM)	2.2	1.8	18,100 (M_w/M_n = 1.3)	insoluble[e]
4	P-(AH-GDM)	0.9	3.0	17,100 (M_w/M_n = 1.3)	soluble
5	P-(AP(OH)-GDM)	0.7	2.7	21,400 (M_w/M_n = 1.5)	soluble
6	P-(AP(OH)-GDM)	4.1	1.8	29,500 (M_w/M_n = 1.8)	insoluble[e]

[a] The compositions of the monomer mixtures in the polymerization feed (HPMA:MA-GFLG-AR-GDM:MA-GG-ONp) were 92.5 : 2.5 : 5.0 for Polymers 1, 4, and 5; 90.0 : 5.0 : 5.0 for Polymer 2; and 85.0 : 10.0 : 5.0 for Polymers 3 and 6.

[b] Determined spectrophometrically (332 nm).

[c] Determined from the ONp^- amount (by absorbancy at 400 nm) released from the polymer by hydrolysis in 0.1 N NaOH.

[d] Molecular weight average (M_w) and polydispersity were estimated by size exclusion chromatography using Superose 6 column (Pharmacia Biotech) and PBS/acetonitrile (7/3 (v/v)), calibrated with poly(HPMA) fractions. The measurements were carried out after Onp groups on the polymers were aminolyzed with 1-aminopropan-2-ol.

[e] Both polymers were soluble in distilled water but precipitated in PBS and in RPMI-1640 cell culture medium.

TABLE II. IC_{50} Doses of Various Free and HPMA Copolymer-Bound Geldanamycin Derivatives[a]

Compound	Free[b] (nM)	Polymer-bound[c] (μM)	Reduction Ratio (c/b)
AP-GDM	136 ± 28	39.6 ± 4.9 (Polymer 1)	292 ± 13
		46.8 ± 5.8[*3] (Polymer 2)	344 ± 15
AH-GDM	735 ± 90[*1]	15.2 ± 1.7[*4] (Polymer 4)	21 ± 1
AP(OH)-GDM	234 ± 39[*2]	21.0 ± 2.0[*5] (Polymer 5)	90 ± 3

[a] The data indicated mean ± SE of n = 8 from two separate experiments (n = 4 at each experiments). All free and polymer-bound GDM derivatives were included in each experiment; IC_{50} doses for free AP-GDM and AP(OH)-GDM have already been reported in reference (12).

[*1] $P < 0.001$ when compared with AP-GDM · HCl.

[*2] $P < 0.05$ when compared with AP-GDM · HCl, and $P < 0.001$ when compared with AH-GDM · HCl.

[*3] not significant when compared with Polymer 1.

[*4] $P < 0.001$ when compared with Polymer 1, and $P < 0.05$ when compared with Polymer 4.

[*5] $P < 0.005$ when compared with Polymer 1.

weight and macromolecular therapeutics is compared based on intracellular concentrations, a different picture emerges. Using the same cell line A2780, Minko *et al.* have shown that the cytotoxicity of HPMA copolymer-bound doxorubicin is at least the same as that of free doxorubicin if compared based on cell-associated doxorubicin (13). This indicates that the reduction in efficacy can be compensated by increasing the dose, maintaining the modified mechanism of action of macromolecular therapeutics.

Of all the P-(AR-GDM)s, P-(AH-GDM) demonstrated the strongest efficacy, however the efficacy of free AH-GDM was not as strong as that of the other AR-GDMs as shown above. Similarly, P-(AP(OH)-GDM) demonstrated higher efficacy than P-(AP-GDM) whereas free AP(OH)-GDM was not as effective as AP-GDM. Conversely, the drug content in P-(AP-GDM) did not have an influence on the efficacy. These data suggests that the efficacy of polymer-bound AR-GDM is affected by other factors relating the AR-GDM structure, not just its intrinsic activity. Several factors influencing the efficacy of P-(AR-GDM)s are discussed below.

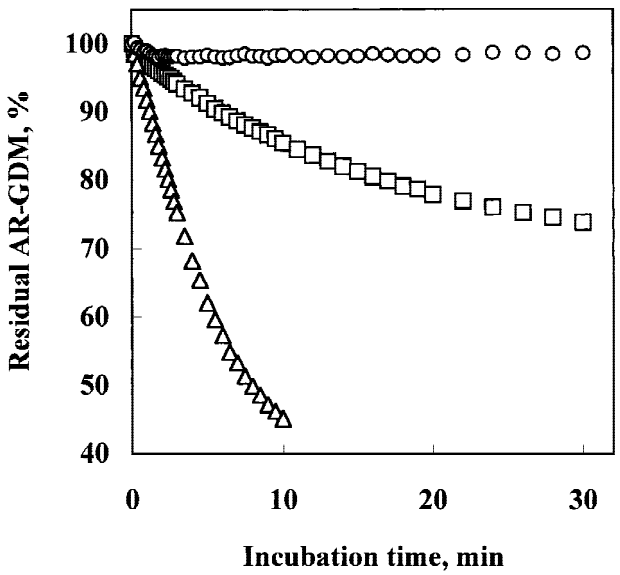

Fig. 1. Stability of AR-GDMs in PBS (pH 7.4) at 37°C. Initial concentration of drug moiety was 8.0 ± 0.5 μM for all AR-GDMs. Squares, AP-GDM; circles, AH-GDM; triangles, AP(OH)-GDM. Data indicate mean from n = 3; SEs are hidden in the symbols.

Factors Influencing the Cytotoxicity of P-(AR-GDM)

After P-(AR-GDM) was added into the cell culture, several steps are involved to express their cytotoxic efficacy (8): Step 1 transport of P-(AR-GDM) from the media to the [vicinity of] cell surface; Step 2, internalization of P-(AR-GDM) by endocytosis; Step 3, fusion of the endosome containing P-(AR-GDM) and a lysosome; Step 4, drug release from P-(AR-GDM) in the secondary lysosome catalyzed enzymatically; and Step 5, transport of the free drugs from lysosome into cytoplasm across the lysosomal membrane.

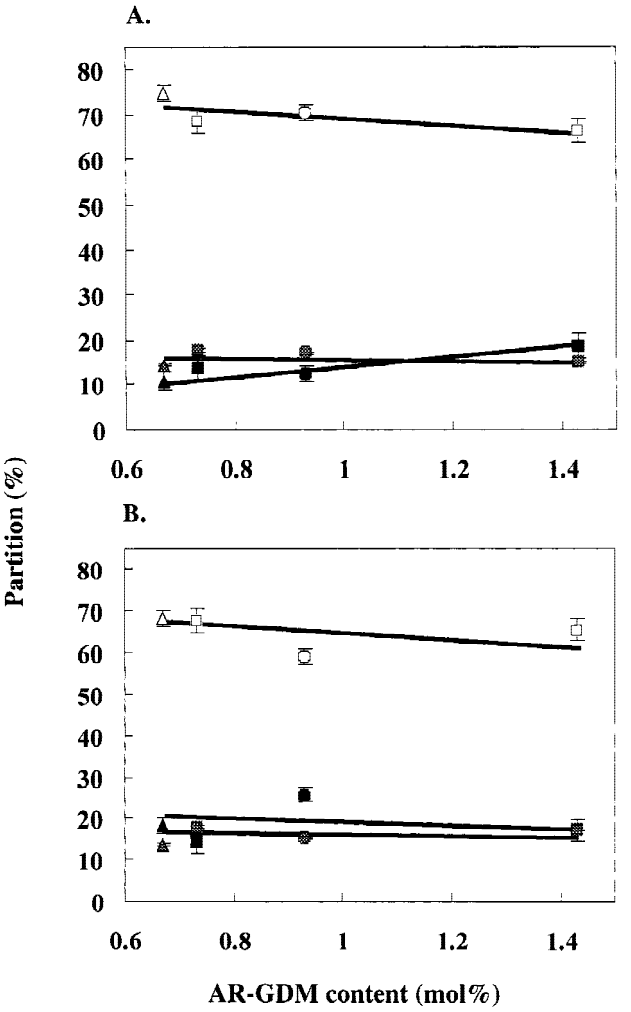

Fig. 2. Influence of GDM derivative content on the partition of P-(AR-GDM) in aqueous two phase systems consisting of PEG_{6000} and dextran T-500. (A), Charge-insensitive systems; (B), charge-sensitive systems. Squares, P-(AP-GDM); circles, P-(AH-GDM); triangles, P-(AP(OH)-GDM. Open symbols, partition in the upper phase; hatched symbols, partition on the interface; closed symbols, partition in the lower phase. Data indicate mean and SE from n = 4.

TABLE III. Drug Release from the P-(AR-GDM) Catalyzed by Cathepsin B[a]

Polymer no.	Structure	Drug release[b] (%)
1	P-(AP-GDM)	8.2 ± 0.5
2	P-(AP-GDM)	6.2 ± 0.2
4	P-(AP-GDM)	21.5 ± 0.3[*1]
5	P-(AP(OH)-GDM)	5.8 ± 0.3

[a] The concentrations of cathepsin B, AR-GDM moiety in P-(AR-GDM), and glutathione were 3 μM, 60 μM, and 5 mM, respectively. Incubation time and temperature were 1 h and 37 °C, respectively.
[b] Data indicate mean ± SE from n = 4.
[*1] $P < 0.001$ when compared with other polymers.

Analysis of these events seems to indicate that Steps 1, 2, and 4 may depend on the structure of macromolecular therapeutics and, consequently, influence the efficacy of P-(AR-GDM)s. Step 1 relates to the stability of drugs, step 2 relates to cellular uptake and subcellular trafficking, and step 4 relates to the biorecognition by lysosomal enzymes and detachment of the drug from the macromolecular carrier. In contrast, step 3 involves only biological events that may be independent of the structure of macromolecular therapeutics. Step 5 could depend on the physicochemical character of AR-GDM (22). However, the properties of the three AR-GDMs are expected to be similar as suggested from the partition coefficient between n-octanol and buffer and the similarity in the structure. In addition, the cytotoxicity of free AR-GDMs suggests that the drugs are able to cross phospholipid bilayer membranes. Consequently, it seems safe to assume that step 5 is not the crucial factor in the efficacy of different P-(AR-GDM).

Drug Stability

Figure 1 shows the stability of AR-GDMs in PBS. AP(OH)-GDM was the least stable of the three. The instability of AP-GDM and AP(OH)-GDM is consistent with previous reports (5,6,14). As expected, due to the protection of the primary amino group during conjugation, very little degradation was observed for all P-(AR-GDM)s during the 24 h incubation (remaining polymer-bound drug contents: 91% for Polymer 1, 98% for Polymer 2, 92% for Polymer 4, and 90% for Polymer 5). The data indicate that AP(OH)-GDM was stabilized most effectively by the conjugation so that the efficacy of P-(AP(OH)-GDM) was relatively high compared to P-(AR-GDM)s. On the contrary, AH-GDM was stable even in the free form, indicating that the higher efficacy of P-(AH-GDM) is attributed to another factor.

Partition in Aqueous Two-Phase Systems

Physicochemical characterization is an indirect but simple and reliable method to estimate the susceptibility to endocytosis. Hydrophobicity (23,24) and electrical charge (25) of substrates may change the mechanism of cellular uptake from fluid-phase pinocytosis (endocytosis) to absorptive pinocytosis (8). To evaluate these two factors we used aqueous two-phase systems (18,26).

First, we adopted the so-called charge-insensitive system that contained 10 mM phosphate anion and 150 mM NaCl to evaluate the hydrophobicity. Figure 2 shows the partition of P-(AR-GDM) in this system. The partition behavior was only slightly dependent on or independent of the drug content and the structure of AR-GDM. In addition, their partition to the upper phase was relatively high (65–75% of total). Aqueous two phase systems consisting of PEG and dextran can detect small differences in the hydrophobicity of relatively hydrophilic materials. It is known that the more hydrophilic the polymer (surface), the more the partition in upper phase that is PEG-rich. For example Xiu *et al.* (26) have reported that partition of Salmonella changes from 1% to more than 90% depending on the strains and mutant-types. There was a close correlation between the partition in the upper phase and the

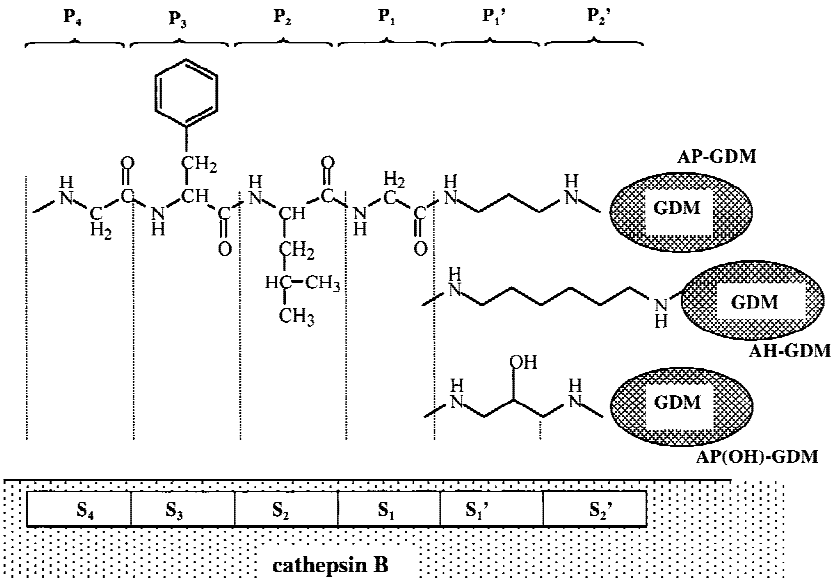

Scheme 2. Schematic representation of the enzyme-substrate complexes of cathepsin B with P-(AR-GDM)s. The S_2' subsite of cathepsin B is located away from the surface and inside the molecule.

phagocytosis of various subtypes of Salmonella by polymorphonuclear leukocytes. Similar results have also been observed in the study of PEG-modified liposomes (27,28). For soluble polymers, Duncan *et al.* (23) have reported that the pinocytosis of HPMA copolymers was enhanced by an increased content of hydrophobic tyrosine residues in HPMA copolymers although the partition behavior is not available. Our results (Fig. 2) suggested that Polymers 1, 2, 4, and 5 possessed similar hydrophilicity.

Next, we compared the partition behavior between charge-sensitive and insensitive systems to estimate the electrical charge of P-(AR-GDM)s. Charge sensitive systems contain higher concentration of phosphate anion (110 mM) but no NaCl; the phosphate anions prefer to distribute in the lower phase (dextran-rich) (18). If materials possess electrical charge, their partition behavior is affected by the unequal distribution of the phosphate anion. As shown in Fig. 2, however, similar partition behavior was observed in both systems. This indicates that the ionic content of all P-(AR-GDM) was negligible.

These observations seem to indicate that the susceptibility to endocytosis is similar in all P-(AR-GDM)s. In other words, it is unreasonable to assume that P-(AH-GDM) possessed a higher susceptibility to endocytosis resulting in higher cytotoxic efficacy.

Susceptibility of GDM Terminated Oligopeptide Side-Chains to Cathepsin B Catalyzed Hydrolysis

Cathepsin B is a lysosomal cysteine proteinase responsible for protein metabolism and the cleavage of the GFLG spacer in the HPMA copolymer-drug conjugates (12). Cathepsin B possesses a specific structural element referred to as the "occluding loop" which contributes to the primed subsites (nomenclature of Schechter and Berger (29) of the substrate binding cleft (30,31). Various P-(AR-GDM) were incubated with cathepsin B and the amount of released drug was measured. As shown in Table III, P-(AH-GDM) demonstrated a substantially larger amount of released drug than the other P-(AR-GDM)s. Drug release was not observed in the absence of cathepsin B for all P-(AR-GDM)s. The mechanism of enhanced drug release from P-(AH-GDM) is suggested as shown in Scheme 2. It is known that the S_2' subsite in cathepsin B is located away from the surface of the molecule, whereas the S_1' subsite is in a shallow binding pocket on the surface (32). This indicates that the steric hindrance of the S_2' subsite could be the predominant factor affecting the formation of enzyme-substrate complex of cathepsin B and P-(AR-GDM). In the cathepsin B-P-(AR-GDM) complex, the hexamethylene spacer likely moved the bulky GDM moiety away from the occluding loop and the S_2' subsite of cathepsin B, rendering the complex formation energetically more favorable. In contrast, the GDM moiety apparently located in this subsite for the other P-(AR-GDM)s. Rapid drug release in the lysosomal compartment might be the reason for the higher efficacy of P-(AH-GDM). The structure of the P_1–P_4 sequence has already been optimized to be the GFLG oligopeptide sequence (12). The linkage between the glycine residue on the C terminus of this spacer and the drug moiety is the main cleavage site. This optimized sequence was used in this study as a spacer between polymer backbone and drug moiety. The data seem to suggest that the structure of primed P positions of P-(AR-GDM) fits well in the active site of cathepsin B.

CONCLUSIONS

The efficacy of HPMA copolymer-bound AR-GDM was strongly dependent on the structure of the 17-substituent. Aminohexylgeldanamycin was found to be a suitable derivative for the drug delivery system based on HPMA copolymers and enzymatically degradable spacers. Stability of drugs in the free form and drug release rate may influence the efficacy of P-(AR-GDM)s. These factors need to be taken into consideration for the design of macromolecular therapeutics of GDM derivatives.

ACKNOWLEDGMENT

This research was supported in part by the NIH grant CA51578 from the National Cancer Institute.

APPENDIX

TABLE IV. Two-Dimensional NMR Data

A) Assignment of AH-GDM · HCl

	Proton	^1H[*1]	^{13}C[*2]
GDM moiety	2-CH_3	1.92, s, 3H	12
	H3	7.02, br s, 1H	128
	H4	6.58, t (J = 10.5 Hz), 1H	126
	H5	5.77, br s, 1H	138
	H6	4.39, br s, 1H	81
	6, 12-OCH_3	3.18, s, 3H	56
		3.21, s, 1H	56
	H7	4.97, s, 1H	80
	7-$OCONH_2$	6.20–6.80, br, 2H	—
	8-CH_3	1.62, s, 3H	13
	H9	5.51, br s, 1H	131
	H10	2.53, br, 1H	32
	10-CH_3	0.92, s, 3H	22
	H11	3.32, br s, 1H	72
	11-OH	6.85–7.00, d, 1H	—
	H12	3.18, br s, 1H	81
	H13	1.49, br s, 2H	33
	H14	1.87, br s, 1H	29
	14-CH_3	0.80, d (J = 6.5 Hz), 3H	14
	H15	2.25, dd (J = 7, 12.5 Hz), 1H	32
		2.48, br, 1H	32
	H19	6.93, br s, 1H	107
	22-NH	9.35, br s, 1H	—
AH moiety	1′-NH	4.18, br s, 1H	—
	1′-CH_2-	2.73, t(J = 7.5 Hz), 2H	38
	2′-CH_2-	1.55, m, 2H	27
	3′-CH_2-	1.25–1.36, m, 2H	26
	4′-CH_2-	1.25–1.36, m, 2H	26
	5′-CH_2-	1.55 m, 2H	29
	6′-CH_2-	3.45, m, 2H	44
	6′-NH_3Cl	7.96, s, 3H	—

[*1] Data of ^1H show the chemical shift, splitting, and number of protons.

[*2] Data of ^{13}C show the chemical shift.

B) Assignment of MA-GFLG-AH-GDM

	Proton	^{1}H	^{13}C
GDM moiety	2-CH_3	1.92, s, 3H	12
	H3	7.02, s, 1H	128
	H4	6.58, t (J = 11 Hz), 1H	126
	H5	5.78, br s, 1H	138
	H6	4.39, d (J = 6 Hz), 1H	81
	6, 12-OCH_3	3.19, s, 3H	56
		3.21, s, 3H	56
	H7	4.98, s, 1H	80
	7-$OCONH_2$	6.20–6.80, br, 2H	—
	8-CH_3	1.63, s, 3H	13
	H9	5.54, br s, 1H	132
	H10	2.53, br, 1H	32
	10-CH_3	0.92, d (J = 6.0 Hz), 3H	23
	H11	3.31, br s, 1H	72
	11-OH	6.8–7.0, br, 1H	—
	H12	3.17, s, 1H	81
	H13	1.40, t (J = 6.0 Hz), 2H	29
	H14	1.82, br s, 1H	23
	14-CH_3	0.81, d (J =8.5 Hz), 3H	14
	H15	2.22–2.28, m, 1H	32
		2.50–2.62, m, 1H	32
	H19	6.8–7.0, br 1H	107
	22-NH	9.33, br s, 1H	—
MA-GFLG moiety	CH_2=(MA)	5.35, s, 1H	120
		5.70, s, 1H	120
	CH_3 (MA)	1.84, s, 3H	18
	_NH of 4 amino acid residues	7.95–8.20, m, 4H	—
	CH_2 (Gly)	3.58–3.68, m, 3H	42
		3.77, dd(J = 6.0, 16.5 HZ), 1H	42
	_CH (Phe)	4.50, m, 1H	54
	CH_2 (Phe)	2.80, dd (J = 9.5, 13.5 Hz), 1H	37
		3.01, t (J = 4.50 Hz), 1H	37
	phenyl (Phe)	7.16, m, 1H	126
		7.20, m, 2H	129
		7.24, m, 2H	128
	_CH (Leu)	4.21, dd (J = 7.5, 14.5 Hz), 1H	52
	CH_2 (Leu)	1.46–1.58, m, 2H	32
	_CH (Leu)	1.46–1.58, m, 1H	24
	CH_3 (Leu)	0.82, d (J = 6.5 Hz), 3H	21
		0.87, d (J = 6.0 Hz), 3H	23
AH moiety	1′-CH_2-	3.05, m, 2H	38
	1′-NH	4.14–4.24, br, 1H	—
	2′-CH_2-	1.46–1.58, m, 2H	30
	3′-CH_2-	1.28, m, 2H	26
	4′-CH_2-	1.63–1.70, m, 2H	30
	5′-CH_2-	1.46–1.58 m, 2H	40
	6′-CH_2-	3.4–3.5, m, 2H	45
	6′-NH	7.63, t, (J = 5.5), 1H	—

C) Assignment of MA-GFLG-AP(OH)-GDM

	Proton	^{1}H	^{13}C
GDM moiety	2-CH_3	1.92, s, 3H	12
	H3	7.032, s, 1H	128
	H4	6.58, t (J = 11 Hz), 1H	126
	H5	5.78, br s, 1H	138
	H6	4.39, br, 1H	81
	6, 12-OCH_3	3.19, s, 3H	56
		3.21, s, 3H	56
	H7 (racemization)	4.97, br s, 0.8H	80
		4.99, br s, 0.2H	80
	7-$OCONH_2$	6.20–6.80, br, 2H	—
	8-CH_3	1.62, s, 3H	13
	H9	5.53, br, 1H	132
	H10	2.55, br, 1H	32
	10-CH_3	0.93, m, 3H	22
	H11	3.28, br, 1H	72
	11-OH[*1]		—
	H12	3.18, br, 1H	81
	H13	1.50, s, 2H	32
	H14	1.85, s, 1H	22
	14-CH_3	0.82, m, 3H	13
	H15	2.29, m, 1H	32
		2.52, br, 1H	32
	H19	6.93, br 1H	107
	22-NH	9.20–9.45, br, 1H	—
MA-GFLG moiety	CH_2=(MA)	5.35, d (J = 1 Hz), 1H	120
		5.69, s, 1H	120
	CH_3 (MA)	1.83, s, 3H	18
	_NH of 4 amino acid residues	7.85–8.20, m, 4H	—
	CH_2 (Gly)	3.56–3.64, m, 1H	42
		3.69, d (J = 6.0 Hz), 2H	42
		3.74, dd (J = 6.0, 16.5 Hz), 1H	42
	_CH (Phe)	4.52, m, 1H	54
	CH_2 (Phe)	2.79, m, 1H	37
		2.98–3.08, m, 1H	37
	phenyl (Phe)	7.16, m, 1H	126
		7.19, m, 2H	129
		7.21, m, 2H	128
	_CH (Leu)	4.26, m, 1H	51
	CH_2 (Leu)	1.50, s, 2H	40
	_CH (Leu)	1.60, m, 1H	24
	CH_3 (Leu)	0.82, d (J = 6.5 Hz), 3H	21
		0.87, d (J = 6.5 Hz), 3H	23
AP (OH) moiety	1′-CH_2-	3.16, m, 1H	43
	1′-NH	4.12–4.20, br, 1H	—
	2′-CH_2	3.70, br, 1H	68
	2′-CH[*1]		—
	3′-CH_2	3.33, br s, 1H	48
		3.52, br s, 1H	48
	3′-NH	7.85–8.20 m, 1H	—

[*1] 11-OH (GDM) and 2′-OH (AP(OH)) were not detected.

REFERENCES

1. L. Neckers, T. W. Schulte, and E. Mimnaugh. Geldanamycin as a potential anti-cancer agent: its molecular target and biochemical activity. *Invest New Drugs* **17**:361–373 (1999).
2. T. Scheibel and J. Buchner. The Hsp90 complex—a super-chaperone machine as novel drug target. *Biochem. Pharmacol.* **56**:675–682 (1998).
3. E. Sausville. Combining cytotoxics and 17-allylamino, 17-demethoxygeldanamycin: sequence and tumor biology matters. *Clin. Cancer Res.* **7**:2155–2158 (2001).
4. J. G. Supko, L. R. Hickman, M. R. Grever, and L. Malspeis. Pre-clinical pharmacologic evaluation of geldanamycin as an antitumor agent. *Cancer Chemother. Pharamcol.* **36**:305–315 (1995).
5. R. Mandler, E. Dadachova, J. K. Brechbiel, T. A. Waldmann, and M. W. Brechbiel. Synthesis and evaluation of antiproliferative activity of a geldanamycin-Herceptin immunoconjugate. *Bioorg. Med. Chem. Lett.* **10**:1025–1028 (2000).

6. R. Mandler, C. Wu, E. A. Sausville, A. J. Roettinger, D. J. Newman, D. K. Ho, C. R. King, D. Yang, M. E. Lippman, N. F. Landolfi, E. Dadachova, M. W. Brechbiel, and T. A. Waldmann. Immunoconjugates of geldanamycin and anti-HER2 monoclonal antibodies: antiproliferative activity on human breast carcinoma cell lines. *J. Natl. Cancer Inst.* **92**:1573–1581 (2000).
7. Y. Kasuya, Z.-R. Lu, P. Kopečková, T. Minko, S. E. Tabibi, and J. Kopeček. Synthesis and characterization of HPMA copolymer-geldanamycin derivative conjugates. *J. Control. Release* **74**:203–211 (2001).
8. D. Putnam and J. Kopeček. Polymer conjugates with anticancer activity. *Adv. Polym. Sci.* **122**:55–123 (1995).
9. J. Kopeček, P. Kopečková, T. Minko, and Z.-R. Lu. HMPA copolymer-anticancer drug conjugates: design, activity, and mechanism of action. *Eur. J. Pharm. Biopharm.* **50**:61–81 (2000).
10. Y. Matsumura and H. Maeda. A new concept for macromolecular therapeutics in cancer chemotherapy: mechanism of tumoritropic accumulation of proteins and the antitumor agent smancs. *Cancer Res.* **46**:6387–6392 (1986).
11. P. Rejmanová, J. Kopeček, R. Duncan, and J. B. Lloyd. Stability in rat plasma and serum of lysosomally degradable oligopeptide sequences in N-(2-hydroxypropyl)methacrylamide copolymers. *Biomaterials* **6**:45–48 (1983).
12. P. Rejmanová, J. Pohl, M. Baudyš, V. Kostka, and J. Kopeček. Polymers containing enzymatically degradable bonds 8. Degradation of oligopeptide sequences in N-(2-hydroxypropyl)methacrylamide copolymers by bovine spleen cathepsin B. *Makromol. Chem.* **184**:2009–2020 (1983).
13. T. Minko, P. Kopečková, and J. Kopeček. Comparison of the anticancer effect of free and HPMA copolymer-bound adriamycin in human ovarian carcinoma cells. *Pharm. Res.* **16**:986–996 (1999).
14. Y. Kasuya, Z.-R. Lu, P. Kopečková, and J. Kopeček. Improved synthesis and evaluation of 17-substituted aminoalkylgeldanamycin derivatives applicable to drug delivery systems. *Bioorg. Med. Chem. Lett.* **11**:2089–2091 (2001).
15. J. Kopeček and H. Bažilová. Poly[N-(2-hydroxypropyl)methacrylamide] I. Radical polymerization and copolymerization. *Eur. Polym. J.* **9**:7–14 (1973).
16. P. Rejmanová, J. Labský, and J. Kopeček. Aminolyses of monomeric and polymeric p-nitrophenyl esters of methacryloylated amino acids. *Makromol. Chem.* **178**:2159–2168 (1977).
17. J. Kopeček, P. Rejmanová, J. Strohalm, K. Ulbrich, B. Říhová, V. Chytrý, J. B. Lloyd, and R. Duncan. Synthetic polymeric drugs. *US Pat.* 5,037,883 (1991).
18. E. Eriksson and P.-Å. Albertsson. The effect of the lipid composition on the partition of liposomes in aqueous two-phase systems. *Biochim. Biophys. Acta* **507**:425–432 (1978).
19. T. Minko, P. Kopečková, V. Pozharov, and J. Kopeček. HPMA copolymer bound adriamycin overcomes MDR1 gene encoded resistance in a human ovarian carcinoma cell line. *J. Control. Release* **54**:223–233 (1998).
20. L. W. Seymour, R. Duncan, J. Strohalm, and J. Kopeček. Effect of molecular weight (M_w) of N-(2-hydroxypropyl)methacrylamide copolymers on body distribution and rate of excretion after subcutaneous, intraperitoneal, and intravenous administration to rats. *J. Biomed. Mater. Res.* **21**:1341–1358 (1987).
21. M. Dvořák, P. Kopečková, and J. Kopeček. High-molecular weight HPMA copolymer-adriamycin conjugates. *J. Control. Release* **60**:321–332 (1999).
22. J. B. Lloyd. Metabolic efflux and influx across the lysosome membrane. In J. B. Lloyd and R. W. Mason (eds.), *Biology of the lysosomes. Subcellular Biochemistry.* Vol. **27**, Plenum Press, New York, pp. 361–386 (1996).
23. R. Duncan, H. C. Cable, P. Rejmanová, J. Kopeček, and J. B. Lloyd. Tyrosinamide residues enhance pinocytotic capture of N-(2-hydroxypropyl)methacrylamide copolymers. *Biochim. Biophys. Acta* **799**:1–8 (1984).
24. Y. Tabata and Y. Ikada. Effect of surface wettability of microspheres on phagocytosis. *J. Colloid Interface Sci.* **127**:132–140 (1989).
25. S. Yasukawa, H. Ohshima, N. Muramatsu, and T. Kondo. Electrostatic interaction of microcapsules with guinea-pig polymorphonuclear leucocytes. *J. Microencapsul.* **7**:179–184 (1990).
26. J. H. Xiu, K.-E. Magnusson, O. Stendahl, and L. Edebo. Physicochemical surface properties and phagocytosis by polymorphonuclear leukocytes of different serogroup of Salmonella. *J. Gen. Microbiol.* **129**:3075–3084 (1983).
27. J. Senior, C. Delgado, D. Fisher, C. Tilcock, and G. Gregoriadis. Influence of surface hydrophilicity of liposomes on their interaction with plasma protein and clearance from the circulation: studies with poly(ethylene glycol)-coated vesicles. *Biochim. Biophys. Acta* **1062**:77–82 (1991).
28. M. C. Woodle and D. D. Lasic. Sterically stabilized liposomes. *Biochim. Biophys. Acta* **1113**:171–199 (1992).
29. I. Schechter and A. Berger. On the active site in proteases. I. Papain. *Biochem. Biophys. Res. Commun.* **27**:157–162 (1967).
30. M. Baudyš, B. Meloun, T. Gan-Erdene, M. Fusek, M. Mareš, V. Kostka, J. Pohl, and C. C. F. Blake. S-S bridges of cathepsin B and H from bovine spleen: A basis for cathepsin B model building and possible functional implications for discrimination between exo- and endopeptidase activities among cathepsins B, H and L. *Biomed. Biochim. Acta* **50**:569–577 (1991).
31. O. Quraishi, D. K. Nägler, T. Fox, J. Sivaraman, M. Cygler, J. S. Mort, and A. C. Storer. The occluding loop in cathepsin B defines the pH dependence of inhibition by its propeptide. *Biochemistry* **38**:5017–5023 (1999).
32. D. Turk, M. Podobnik, T. Popovic, N. Katsunuma, W. Bode, R. Huber, and V. Turk. Crystal structure of cathepsin B inhibited with CA30 at 2.0 Å resolution: A basis for the design of specific epoxysuccyl inhibitors. *Biochemistry* **34**:4791–4797 (1995).